Global Journal of Scientific Researches

Available online at gjsr.blue-ap.org
©2017 GJSR Journal. Vol. 5(3), pp. 44-52, 30 June, 2017
E-ISSN: 2311-732X

Determine relating subsidence and extraction of oil in naft-Shahr oil area by INSAR method

Jafar Rafiee[1*] and Morteza Sedighi[2]

1. Department of civil engineering geodesy, Iran
2. Islamic Azad University, Ahar, Iran

Corresponding Author: Jafar Rafiee

Received: 25 May, 2017 *Accepted: 6 June, 2017* *Published: 30 June, 2017*

ABSTRACT

Subsidence as a geometric hazard has reached a critical level in some parts of the Iran in recent years (Behniafar and et al, 2010). Gradual and sudden subsidence of ground is affected by natural the ground mainly due to the extraction of fluids such as water and oil (Ranjbar and et al, 2009) Subsidence is continuation for long periods of time can cause irreparable damage to building, road, bridge, pipeline and transmission lines. Different method such as precise leveling, the GPS and remote sensing technology are utilized to monitor subsidence (Akhundi.M, 2005). The use of remote sensing in different sciences related to geology is more common compare to the ground method because of the wide courage of satellite images, their accessibility and update as well as their low cost. One of the uses of INSAR control and monitor the displacement of earth crust as the result of phenomena such as earthquake, landslide and subsidence. For monitoring this phenomenon fourteen satellite images from 2004 to 2010 have been used, furthermore the DEM of the area, which was previously prepared, was also employed, in order to process the image SARPACE software in the platform of EN.v14.8 was used. Finally, the rate of subsidence average was calculated through adjustment by least it was equal 10 centimeter per year. The overall process was done by forming is interfrogram and performing filtration.

Keywords: *Subsidence, INSAR, interfrogram, naft-shahr.*

INTRODUCTION

Withdrawal of hydrocarbon fluid from reservoirs with high compression and low permeability can gradually cause surface deformation and subsidence, which in turn can cause considerable damages and expenses. To calculate the level of subsidence, a variety of methods are used, the most important of which is (1) use of GPS, (2) precise leveling, (3) (InSAR) interferometry technique in remote sensing. One of the applications of GPS is displaying the displacement of the earth's crust either in horizontal or vertical direction, which involves control points with high precision and some limitations because of ground stations. Another method is the use of precise leveling which involves iteration of first-rank leveling observations, as it does not seem economical to areas with dense vegetation. But interferometry technique has certain advantages in measurement and displacement of earth crust, including high sensitivity to dynamic changes, high spatial resolution power and vast coverage, lack of a need for ground control points. By using some SAR images of dynamic changes in an area, we can obtain interferogram of changes with a precision of about a millimeter, as well as calculating horizontal and vertical displacement after ground subsidence. Interferometry is a method of using ground return signal phases in two SAR images taken with a time delay in order to derive altitude and data relating to surface changes. 14 images between the years 2004 and 2010 were used, and this phase difference can include atmospheric effects, topography, etc. It is evident that the effect of the identified factors should be eliminated in order to obtain an accurate result.

Imaging geometry of SAR

SAR system is a radar system that sends microwave radiation to the target (ground level) and measures the phase of the return signal.

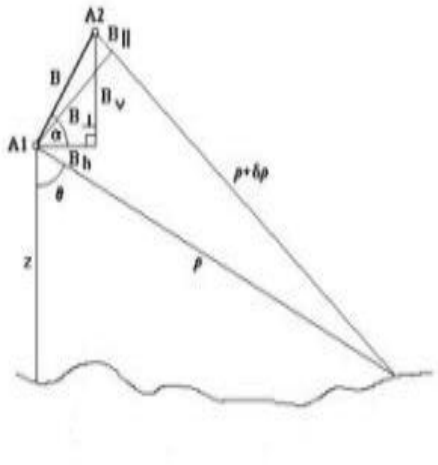

Figure 1. Imaging geometry of SAR

Distance difference between two mages is calculated in order to create interferogram and height changes of two corresponding pixels as follows;

$^{\varphi} = \frac{4\pi\delta\rho}{\lambda}$ (1)

λ : wavelength

δρ : distance difference between target and sensor

ϕ: phase difference of measured height

ha= $\frac{\boldsymbol{\rho\lambda\sin\theta}}{\boldsymbol{2B\cos(\theta-\alpha)}}$ (2)

θ: look angle in nadir

α: Baseline orientation angle

Method

1. INSAR and how to use it

Use of radar interferometry is common to the investigation of phenomena namely landslide, earthquake, subsidence, etc. In this method, the possibility of creating interoferogram derived from phase difference is provided by using repeat track and InSAR technique

(ϕ) phase difference formula:

$\boldsymbol{\phi} \equiv \sum(\Delta\boldsymbol{\varphi}[\mathbf{orb}] + \Delta\boldsymbol{\varphi}[\mathbf{topo}] + \Delta\boldsymbol{\varphi}[\mathbf{atm}] + \Delta\boldsymbol{\varphi}[\mathbf{N}] + \Delta[\boldsymbol{\varphi}\mathbf{def}])$ (3)

(*V.K.Dang et al, 2014).*

Phase difference is because of circuit error which is either due to incomplete modeling of satellite dynamics in space or the residual effects of disturbances and acts of selective ability (SA), which can be reduced by precise circuit data or determination of differential situations in short distances INSAR is an intentional error made to orbiting satellites by United States Department of Defense *(Yahya. J and et al, 2009)*

Δφ[topo]: composed of two components Δφ[flat] and Δφ[elevation].

$\Delta\boldsymbol{\varphi}[\mathbf{flat}] = \frac{\boldsymbol{-4\pi}}{\boldsymbol{\lambda}}\frac{\mathbf{BnS}}{\mathbf{Rtan\theta}}$ (4)

$\Delta\boldsymbol{\varphi}[\mathbf{elevation}] = \frac{\boldsymbol{-\Delta q}}{\boldsymbol{\sin\theta}}\frac{\mathbf{Bn}}{\mathbf{R0}}\frac{\boldsymbol{4\pi}}{\boldsymbol{\lambda}}$ (5)

The two above terms (topography) can be solved with a digital elevation model (DEM) *(Yahya. J and et al, 2009)*

Δφ[atm]: atmospheric phase difference consists of two components namely ionosphere refraction and tropospheric refraction. Ionosphere refraction: includes various layers of atmosphere from about 50 km to 1000 km above the ground surface which is a dispersive medium and signals received from satellites sustain delay or priority when passing through this layer. The ionosphere refraction is dependent on the number of free electrons per unit area of signal path. Tropospheric refraction: troposphere is referred to as part of atmosphere which lies from above the ground surface to an altitude of approximately 10 km. troposphere layer is a non-dispersive and independent of frequency as it is dependent on factors such as temperature, humidity, pressure, and landform on signal path. Atmospheric component (atmospheric phase difference) can be revised by using neutralized duplicate

images or using other resources such as GPS. $\Delta\boldsymbol{\varphi}[\mathbf{N}]$**:** modeling components derived from noise is very difficult and there is no conventional way to remove it. In this paper, in Sarscape noise error has been reduced remarkably by using Goldsion filter**.** $\Delta\boldsymbol{\varphi}[\mathbf{def}]$**:** as a matter of fact, our main goal is to derive the amount of displacement of measured phase by removing or reducing other effects of components to a minimum.

$$\Delta\boldsymbol{\varphi}[\mathbf{def}] = \frac{4\pi\Delta R}{\lambda} \quad (6)$$

$\Delta\mathbf{R}$**:** satellite distance from earth based on satellite line-of-sight. $\boldsymbol{\lambda}$**:** Wavelength

2. Data

We used 14 images of ENVISAT satellite between the years 2004 and 2010.

2.1. Sources of subsidence

2.2: subsidence caused by landform; subsidence can vary according to landform and type of geological strata in a region and the level of permeability or impermeability.

2.3: subsidence caused by human activities; urban sprawl—exploitation of groundwater and oil resources etc.

2.4: different methods of monitoring crustal deformation; Global Positioning System (GPS)- precise leveling

Photogrammetry: a method based on parallax. VLBI technique; mostly used in earthquake optic remote sensing SLR technique

Radar interferometry: radar imaging with synthetic aperture radar is a coherent imaging method by means of microtonal waves with a long exposure. In other words, SAR is a general image system which is used for improving image resolution by setting an artificial antenna.

In radar interferometry two SAR images are synthesized in two different circuits in different times from a specific area. Phase signal difference of both images is obtained in the following equation;

$$\boldsymbol{\Phi = \Phi 1 - \Phi 2 = \frac{4\pi}{\lambda}\ (R2 - R1)} \quad (7)$$

Interferometry is very sensitive to R2—R1

φ1= phase of first SAR image Master

φ2= phase of second image SLAVE

R1= satellite distance from ground surface in the first image

R2= satellite distance from ground surface in the second image

λ= wavelength

interferometry phase is determined to be the argument of normal interferometry phase(*(Tazio Strozzi.U. W, 2001)*

Coherence level between the first image and the second image is obtained from the following equation:

$$\mathbf{t} = \frac{(\mathbf{S1.S2}^*)}{(\mathbf{S1.S2}^*)(\mathbf{S1.S2}^*)} \quad (8)$$

t= image correlation coefficient (coherence)

S1= first image

S2= conjugate of the second image

Interferometry phase is sensitive to topography component and level of correlation between two images (coherence), and delay and precedence in the atmosphere and noise phase are the main sources of error(*Vajedian.S, 2010)*

To remove sources of error and perform processing phases, we use a linear model(*(Tazio Strozzi.U.W, 2001)*

$$\mathbf{t} = \frac{4\pi}{\lambda}\mathbf{B}_{||} + \frac{4\pi}{\lambda}\mathbf{R}_{\mathbf{dis\,p}} + \frac{4\pi}{\lambda}\mathbf{R}_{\mathbf{atm}} + \boldsymbol{\Phi}_{\mathbf{noise}} \quad (9)$$

$\mathbf{B}_{||}$: As per baseline (separation between two antennas, distance between two points of images 1 and 2)

$\mathbf{R}_{\mathbf{disp}}$: Distance according to satellite line-of-sight

$\mathbf{R}_{\mathbf{atm=}}$ Changes made to the phase along the way under different climatic circumstances in two SAR images.

Interferometry phase (t) does not currently change from 0 to 2π. In order to fix this, we unwarp interferometry phase.

To this end, we calculate the differential from the above equation relating to height changes (Z).

Differential of first equation term

$$\frac{\mathbf{B}_{\perp}}{\mathbf{r sin\theta}} = \frac{4\pi}{\lambda}\frac{\partial\Phi}{\partial z} \quad (10)$$

R: satellite distance from the ground

θ: declination angle

B_⊥: component perpendicular to the baseline to satellite line-of-sight

If the baseline is small enough, R is assumed to be equal for both situations. Now, for ERS SAR images with a wavelength of λ= 5.66 cm and the declination angle θ: 23 and R in the range R=853 Km.

The above equation is revised as follows;

$$\frac{\mathbf{B}_{\perp}(\mathbf{m})}{\mathbf{1500^2}}\ \frac{\partial\Phi}{\partial z} \quad (11)$$

It is 50 m for perpendicular baselines and height changes is 188 m in period 2π(*Bamler.R, 1998)*

For 50 m perpendicular baselines, phase error is about 0.11 π.

Though topographic effects are so minimal in interferometry phase with small perpendicular baselines, they are not negligible in regard to calculation of subsidence with very low range.

The differential of the first term of equation 3 in proportion to Y (FLAT component) based on range

$$\frac{B_{\perp}}{R \tan\theta} \frac{4\pi}{\lambda} \cdot \frac{\partial \Phi}{\partial Y} \quad (12)$$

The differential of the first term of equation 3 in proportion to X (altitude component in Azimuth)

$$\frac{\partial B_{||}}{\partial x} \frac{4\pi}{\lambda} = \frac{\partial \Phi}{\partial x} \quad (13)$$

In this equation, $\frac{\partial B_{||}}{\partial x}$ represents $\mathbf{B}_{||}$ changes with respect to line-of-flight and, in consequence, no parallel circuits (deletion of circuit error)

$\mathbf{r_{disp}}$ = phase term related to displacement for scattered center in regard to look vector of radar, in that if it is transferred in perpendicular direction (perpendicular component), it is $\mathbf{r_{vert}}$; in this case deformation is calculated in perpendicular direction (of subsidence) with the following equation:

$$\frac{r_{disp}}{\cos\theta} = \mathbf{r_{vert}} \quad (14)$$

3: Location of study area

The city of Naft-shahr is located in Iran in the west part of Kermanshah.

In terms of geographic coordinates, Naft-shahr is at 32.9886 degrees north and 45.5019 degrees west and 139 m above sea level.

3.1: history of exploitation and level of annual exploitation of hydrocarbon fluid from the study area:

For the first time, British people exploited the oil field under 1933 contract and Angolo-Persian Oil Company started working on the basis of this deal which is actually a revision of 1901 D'Arcy concession. Kermanshah Refinery was founded in 1935 with an annual capacity of one hundred thousand tons from about 18 wells with an average depth of 250 to 400 meters, and in the same year, the line of oil transfer from Naft-shahr to Kermanshah was constructed. In recent years, a daily average of eleven to twenty thousand barrels is withdrawn from reservoirs of Naft-shahr.

4. Stages of displacement map processing and preparation

4.1. Selection of image:

To preview changes in the ground surfaces, a type of paired image from a special area at different times is used; in this research, the image of two previous time spans is taken as MASTER and the second image as SLAVE (one of the images is taken as MASTER and changes of the second image SLAVE are measured with respect to MASTER image).

4.1.1: selection of paired images from ENVIASAT sensor

Proper and optimal selection of paired radar pictures for interferometry is viewed as the foremost and most important steps in the operation of radar interferometry. In this regard, the frequency of the sensor, spatial perpendicular baseline, temporal baseline, spatial overlap and spectral overlap with respect to (Azimuthally) flight are considered the basic factors in the choice of paired images. Envisat sensor has transmitter and receiver antennas operating in band C (with a wavelength of 6.5 cm). The use of this sensor yields satisfactory results for interferometry in areas where there is dense vegetation due to greater permeability of coverage level and more effective backscattering from ground level. Due to certain features of the area, Envisat images during the period 01/02/2004 and 07/09/2010 were used. In SARPACE with ENVI platform, interferometry with DEM (digital elevation model); that is to say, interferogram is actually the same images taken from phase difference between two radar images and demonstrating their changes, so topography error and land flatness are skipped with DEM of the area.

5: Calculation of image baseline

5.1: definition of baseline:

Baseline is actually the spatial distance between the first image and the second image, in that the shorter a baseline, the better processing will be; that is to say, $\frac{\text{Normal Baseline}}{\text{Critical Baxeline}}$ should be less than 500.

5.2: critical baseline:

It is a baseline that its coherence is zero, i.e. there is no data image.

$$\text{Bctit} = \rho\Delta\theta\ \Delta\rho\ \perp\ = \frac{\lambda\rho\tan\theta}{n\Delta\rho} \qquad n=1,2 \quad (15)$$

Note: the longer the wavelength or the better the resolution, the longer the critical baseline. As a matter of fact, interferogram declines in sensitivity to baseline, causing data to be deleted.

$$\frac{\partial \phi crit}{\partial \rho} = \frac{\partial \phi crit}{\partial \theta}\frac{\partial \theta}{\partial \rho}$$

$$\frac{2n\pi}{\lambda} Bcrit \frac{1}{\rho tan\theta} = \frac{2\pi}{\Delta\rho} \qquad (16)$$

critB: critical baseline **θ:** declination angle **λ:** wavelength

5.3: condition of radar interferometry

The surface of an area of the ground which is shown with a radar image pixel consists of hundreds of geographical features. Each of the features contributes to the formation of a pixel with a different reflection coefficient.

Assuming that L represents ground pixel length perpendicular to the axis of satellite flight (20 m for ERS-1), λ is radar wavelength (65 mm for ERS-1) and θ_2 ، θ_1 represents declination angles for image 1 and image 2 respectively, going and returning difference between targets of the two ends of a pixel is $2L\sin\theta$. Thus, the main condition of interferometry is shown as inequality (8).

$2L (\sin \theta_1 - \sin \theta_2) < \lambda$ (17)

The condition of radar interferometry is that the phase difference of corresponding pixels of two images should not exceed half of wavelength. This condition reduces separation (distance) between circuit path of satellites to 1 km or less in the course of taking two images. Fortunately, circuits of satellite are designed in the way that it repeats imaging equally after the time period (circuit circle), and generally this condition applies to them.

Local slope is influential in these conditions. In the case of approaching the minimum interferometry (8), even a gentle slope can eliminate fringes with wrong justifications. According to equation (8), steep declination angle can make it harder for high resolution and short wavelength of all conditions. Moreover, look direction should be the same for two images.

Registration:

At this point, geometrical errors relating to location difference of sensing antenna will be removed in the course of imaging an area. Stages of this method are as follows;

Calculation of overlap level in two images and calculation of coordinates of a series of points in the shared point of the two images in SLAVE image

Determination of pictorial coordinates of the same points in MASTER image by using correspondence evaluation methods

Determination of connection function for connecting two images

Transfer of SLAVE image points to MASTER image, resampling, which is the interpolation of Master image so that these points can fit into a regular grid in Master image in the closest node.The image emerging from phase difference between two radar images and representing their changes and is shown with dint link, and has a great deal of noise which needs to be filtered.

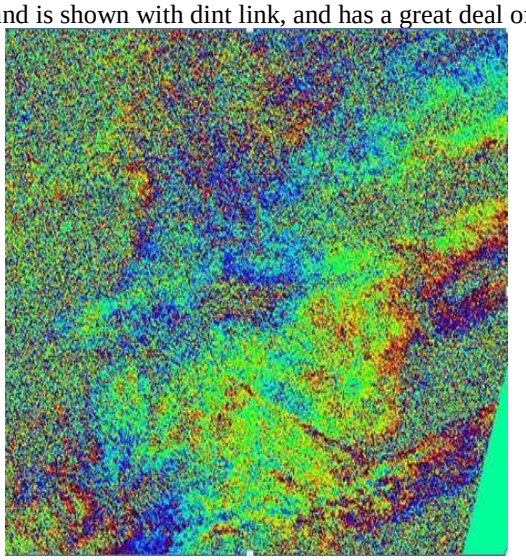

Figure 2. Interferogram image without application of filter

Areas with high noise are areas with low coherence

Fringes created in the interferogram represent changes of ground surface at the time of capturing two pictures.

In the raw image, effects of noise and atmosphere, which are low in value, and topography of land flatness are shown.

5.4: applying filter (filtration)

In order to blunt curves and remove high level of noise, final interferograms are filtered, so that the noise that occurs during the process of phase unwrapping can be reduced. To remove the noise and improve interferometry, three kinds of filter can be used. The first one is adaptive. This filter makes no change in a phase at all. In research in that the goal is to prepare DEM or measure the level of subsidence, the use of this filter is recommended. The second is Boxcar; the state between the first and second filter. The third filter is Godstein; this induces great change in phases and wave correlation as opposed to adaptive filter. When the goal is to offer an output showing changes of wave solidarity, the use of this filter is recommended.

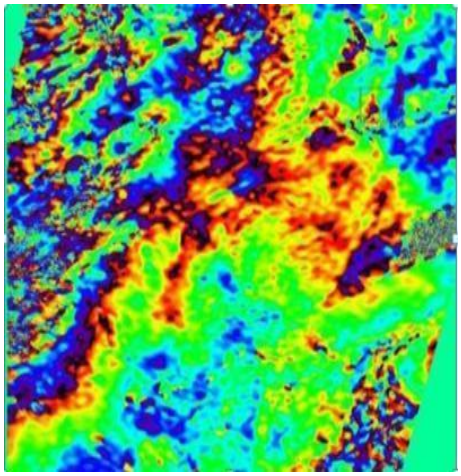

Figure 3. Filtered interferogram image

5.5: Coherence:

Coherent image is an image created by power correlation of two coordinated images. This image represents correlation index of signal power values in two images taken at two different times. The correlation value varies from 0 to 1, which is effective in the quality of interferometry process. In general, if the value of this index is low for a pair of images used in interferometry, it means that this pair is not good enough for interferometry (Kames, 2006). Coherence suggests the level of phase correlation between two images, in that the higher the level of coherence, which is close to 1, the more the coherence between two images is seen, and usually cliffs have the highest coherence, the closer the number to zero, the more the lack of coherence between images is estimated. Typically, water has this characteristic. In the research of the study area, there is a lake in Iraqi territory where images are seen with high noise and coherence is seen in black in images.

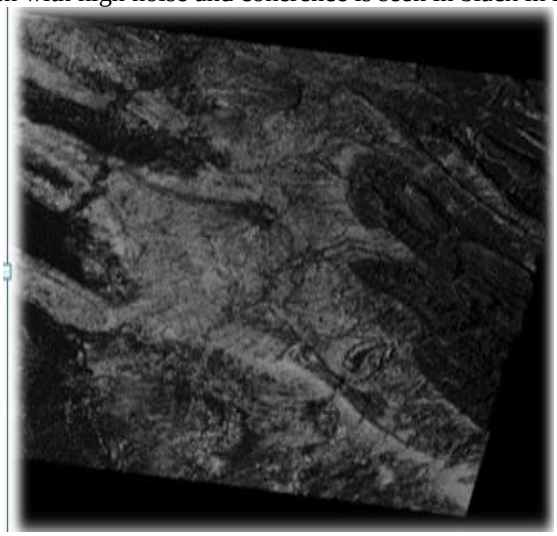

Figure 4. Coherence image

$$\gamma = \frac{|\sum S1(X).S2(X)|}{\sqrt{|\sum S1(x)^2|}.\sqrt{|\sum S1(x)^2|}} \quad (18)$$

S1 (x): first image
S2 (X): the conjugate of the second image

5.3: phase-unwrapping process

In this phase, existing discontinuities of two phases in areas with high coherence are eliminated; that is, interferogram phase which is rotational, from 0 to 360 degrees e.g. 360—180—360—180—0, becomes continuous e.g.

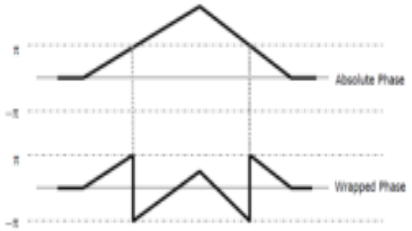

Figure 5. Ideal interferometry phase and unwrapped phase

If there is no noise, it is so easy to unwrap a phase. In figure 4 the phase of ideal interferometry is shown. It shows that phase changes from zero to 2π and returns to zero and this process is iterated. But due to noise that exists in InSAR interferogram phases (fig. 4), unwrapping becomes difficult. In order to convert unwrapped phase to a real phase, we need a series of ground control points (GCPs).

5.6: choice of GCP

Before determining the level of displacement, we choose a series of control points with the minimum displacement (assuming that they have no displacement) and they need to meet the following conditions.
High coherence and no displacement
With correlation points; in this case, the points are introduced and stored as vector

5.7. Converting phase to displacement map

Each cycle of 2 π phase value in differential interferometry is equal to half the wavelength used in radar system, suggesting the level of displacement with respect to antenna line-of-sight. After additional phase refinement and correction, now we can convert absolute phase power to displacement values or displacement map and reference ground. The resulting map entails positive values at this point concerning displacement of ground surface toward radar sight direction (uplift) and negative values suggesting ground surface remoteness from sensor in the direction of radar sight (subsidence). At this point, using this method and deletion of pixels with positive values (uplift) and negative pixels remaining, the map pf subsidence is determined.

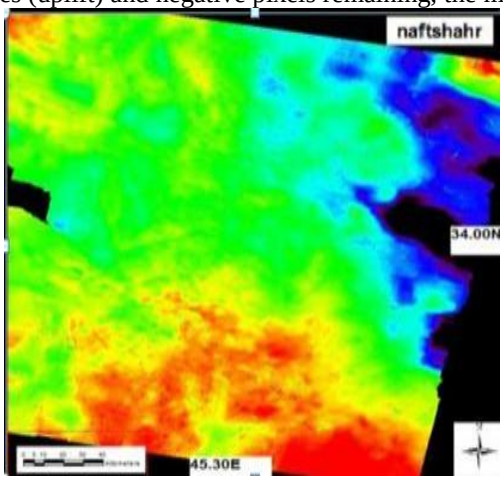

Figure 6. Displacement map

5.8.: estimation of subsidence displacement

Having obtained interferograms, we perform unwrapping on them by means of Sarscape software and convert phases to the extent that it suggests crustal displacement. These changes are calculated both in satellite line-of-sight and vertical and horizontal

directions. By reviewing displacement maps in that subsidence occurred, we note that these areas have one point, the center of subsidence. As we go away from this point, the level of changes will be less and less. The greater the amount of subsidence, the greater the rate of numerical changes is shown. In an attempt to let each pixel has a proper location on the ground in the image, the map of changes is geometrically corrected by circuit data of satellite, and the obtained interferogram is taken as reference ground after removal of errors. Subsequent to computer processing, X= (ATPA)-1AT PY was used with the least square by means of Sarscape specialized software program in ENVI platform and application of interferometry methods using time-series analysis. This method is implemented with an algorithm, dealing with the estimation of integration phase at the time of capturing images. The final map is the average rate of subsidence in the oil field of Naft-shahr, which is the result of time-series analyses from 2004 to 2011 from fourteen images and ten interferograms for the entire region. The level of subsidence in the study area is 7 to 13 cm a year, but the average rate is 10 cm a year.

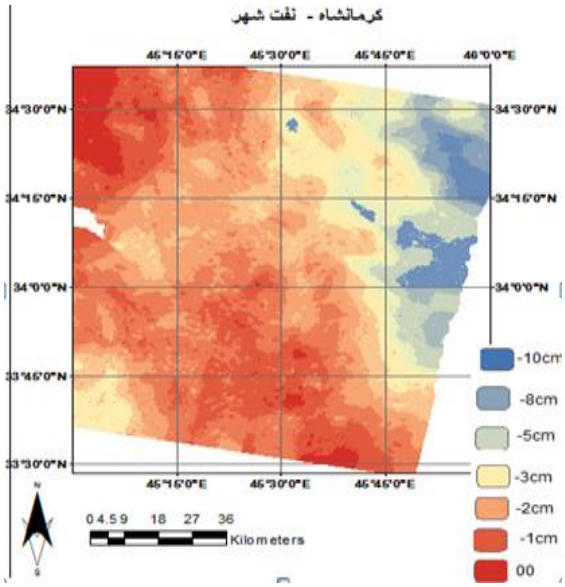

Figure 7. Final map with average rate of 10 cm subsidence a year

Conclusion:

Interferograms resulting from radar image processing during 2004-2010 confirm the occurrence of subsidence phenomenon with an average rate of 10 cm per year around the wells being exploited, in that if this withdrawal continues in the same manner, the risk of a serious subsidence is grave. There are a variety of monitoring methods for subsidence, including precise leveling and use of GPS system as well as radar interferometry, that each has advantages and disadvantages. Since vast areas need to be normally surveyed and controlled in an effort to monitor subsidence and land methods are time-consuming and costly and considering the fact that interferometry method is a good and highly accurate method and due to vast coverage of satellite images and their availability, we can study and control ground surface displacements by benefitting from this technique. Radar interferometry phase is highly sensitive to topography and coherence components, which is why DEM of the area is used in order to remove errors of topography. In order to maintain coherence, we can use images in short time spans and choose small baseline as much as possible. Because of oil and gas withdrawal from underground reservoir surface, subsidence has taken place in Naft-shahr.

REFERENCES

[1] Akhundi, M. (2005). Displaying subsidence of landslide caused by oil exploitation by using SAR interferometry in remote sensing. A conference on Global Positioning Geometrics. Iran.
[2] Amighpey, M. Arabi, S. Talebi, A. Jamor, Y. Study of subsidence areas in Iran by using precise leveling. Iran.
[3] Bamler,R, and P, Hartl, 1998, Synthetic aperture radar interfrometry Inverse problems, 14 R1-R54.
[4] Behniafar.A, Ghanbarzadeh,H. (2010). Study of factors associated with subsidence in Mashhad Plain and its geomorphic consequences. Journal of Geography and urban planning, Zagros Landscape, year II, issue 5, autumn 89, pp. 131-144.
[5] Haghighatmehr, P. Valadanzoj, MJ. (2012) time-series analysis of Hashtgerd subsidence by using radar interferometry and Global Positioning System. Journal of Earth Science, year 22nd, issue 85, pp. 105-114.
[6] Moher, G, and S, N, Madsen, 1999, Error analysis for interfrometric SAR measurement of ice sheet flow, proceeding of IGARSS 99, 28 June – 02 July, Hamburg, Germany.

[7] Ranjbar, M. Jaafari, N. (2009). Study of factors associated with land subsidence in Eshtehard Plain. Journal of Geography (scientific-research edition of Iran Association of Geography), new volume, year 6th, issues 18 and 19, pp 155-166.
[8] Tazio Strozzi, U. W. (2001, nov 11). Land Subsidence monitoring with Deferential SAR interfrometry. pp. 1261-1270.
[9] Vajedian, S. (2010). Radar imaging with artificial aperture. University of Tehran. Faculty of Civil Engineering, Surveying. Iran.
[10] V.K.Dang et al, Recent land subsidence caused by the rapid urban development in the Hanoi region (Vietnam) using ALOS INSAR data, Hazard Earth syst.Sci,14, 2014, 657-674.
[11] Yahya, J. (2009). Course pamphlet on systems of satellite positioning in Engineering Surveying. Iran.